PROCEEDINGS OF SCIENCE

Flavor Oscillation with A Million Atmospheric Neutrinos

C. A. Argüelles, P. Fernández, Ivan Martínez-Soler, M. Jin
E-mail: carguelles@fas.harvard.edu, pablo.fernandez@dipc.org, imartinezsoler@g.harvard.edu, miaochenjin@g.harvard.edu

Atmospheric neutrinos have played a crucial role in discovering neutrino oscillations, the only evidence of non-zero neutrino masses. Even now, they contribute significantly to our understanding of neutrino oscillations and mixing in the lepton sector. This talk analyzes the expected sensitivity of current and near-future water(ice)-Cherenkov atmospheric neutrino experiments. In this first in-depth combined atmospheric neutrino analysis, we carefully review the synergies and features of Super-Kamiokande, IceCube-Upgrade, and ORCA to examine the potential of joint analysis. By a detailed study of the current shared systematic uncertainties arising from the shared flux and neutrino-water interactions, and the systematic uncertainties of each experiment, we probe that the octant of θ_{23} can be resolved at 99% C.L. and the neutrino mass ordering above 5σ by 2030. Additionally, we assess the capability to constraint θ_{13} and the CP-violating phase (δ_{CP}) in the leptonic sector providing vital information for next-generation neutrino oscillation experiments.

Corresponding authors: Ivan Martinez-Soler[1*]
[1] *Department of Physics and Laboratory for Particle Physics and Cosmology, Cambridge 02138, MA, United States*

[*] Presenter

The 38th International Cosmic Ray Conference (ICRC2023)
26 July – 3 August, 2023
Nagoya, Japan

PoS(ICRC2023)1140

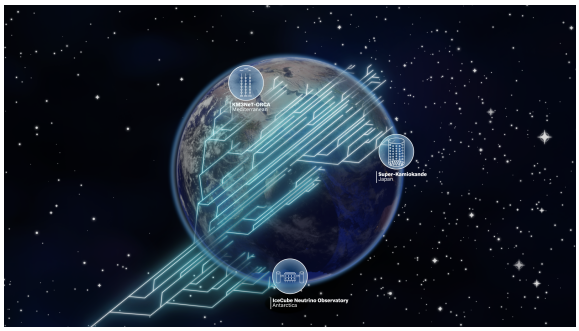

Figure 1: ***Illustration of the atmospheric neutrino flux production.*** Locations of experiments used in this work are shown.

1. Introduction

The collision between cosmic rays and atmospheric nuclei results in the generation of electron and muon neutrinos through the decay of charged mesons formed during the interaction. These atmospheric neutrinos have played a vital role in the discovery and comprehension of neutrino oscillations, mainly because they cover an extensive range of baseline to energy ratios (L/E_ν) spanning ten orders of magnitude. The baseline L varies from 15 km to 12700 km, while the neutrino energy ranges from $O(10^{-2})$ GeV to $O(10^5)$ GeV:see Fig. 1 for an artistic depiction of the production of atmospheric neutrinos and the detectors employed to observe them.

The extensive program that utilizes accelerator, reactor, and solar neutrinos to study neutrino evolution still carries some uncertainties. In this study, we demonstrate how atmospheric neutrinos can contribute to enhancing our understanding of the significant remaining unknowns. To achieve this, we employ a data combination approach, incorporating current and upcoming atmospheric neutrino experiments. Our focus lies specifically on the synergy between SuperK, IceCube Upgrade, ORCA, and HyperK. For the first time, we have developed the necessary tools to perform a comprehensive joint analysis, utilizing the most realistic publicly available simulations for each experiment. This enables us to conduct an in-depth examination of these three experiments, considering detailed descriptions and implementations of detector responses, as well as accounting for common systematic uncertainties. Within this work [1], we address questions falling into three categories: determining neutrino oscillation parameters, establishing the neutrino mass spectra, and measuring the CP-phase in the lepton sector. Furthermore, the combination of these experiments serves as an initial input for the next generation of neutrino experiments.

The Pontecorvo-Maki-Nakagawa-Sakata (PMNS) matrix establishes a connection between the flavor and massive neutrino states. Precisely determining the lepton mixing parameters holds immense importance in comprehending neutrino evolution and can potentially hint at the existence of a concealed flavor symmetry [2]. Additionally, observing significant CP-violation in the neutrino sector could provide an explanation for the baryon asymmetry observed in the early universe through a sphaleron process [3]. Furthermore, the determination of the neutrino mass spectrum in the coming years will have a profound impact on experiments aiming to ascertain the absolute scale of neutrino masses [4], distinguish between the Dirac or Majorana nature of neutrino masses [5], and even gain insights into the evolution of the universe [6].

2. Atmospheric neutrino flux

The cosmic ray spectrum encompasses energies ranging from MeV to EeV [7]. It primarily consists of free protons (approximately 80%) and bound nuclei (approximately 20%). When cosmic rays interact, charged mesons and muons are generated, which subsequently decay and produce a flux of electron and muon neutrinos. At lower energies, this neutrino flux follows the cosmic-ray spectrum but softens by around one spectral index unit as the mesons begin interacting in the atmosphere. The distribution of neutrino flux with respect to zenith angle exhibits an enhancement for horizontal directions. This enhancement is due to the longer paths the mesons have to traverse before reaching Earth, along with the spherical geometry of the volume where neutrinos are produced.

The flavor composition of atmospheric neutrinos undergoes changes depending on their energy. The presence of Earth leads to the absorption of mesons and muons, which in turn enhances the muon component of the initial neutrino flux. If all parent particles are capable of decaying, we would anticipate a ratio of $(\nu_e + \overline{\nu}_e)/(\nu_\mu + \overline{\nu}_\mu) \sim 1/2$ to be approximately 1/2. However, as the energy increases, this ratio gradually decreases.

At lower energies, the presence of the Earth's magnetic field can result in the trapping of low-energy charged mesons. This leads to an enhancement of neutrinos and anti-neutrinos at these lower energies. Additionally, the trajectory of primary cosmic rays that reach Earth is influenced by magnetic effects, resulting in an east-west asymmetry [8]. Moreover, when mesons are trapped, multiple scattering can occur, which affects the neutrino-to-antineutrino ratio. However, as the energy increases, the significance of the geomagnetic effect diminishes, and the neutrino component of the flux becomes dominant.

The calculation of the atmospheric neutrino flux involves several sources of uncertainty, which can be attributed to four main factors: the incident cosmic-ray flux, the model used for hadronic interactions, the atmospheric air density profile, and the magnetic effects at low energies. In order to account for all these uncertainties, we adopt the flux parametrization described in Ref. [9].

3. Neutrino water cross-section

The experiments analyzed in this study share a common target, which is water, although they operate at distinct energy scales to measure neutrino interactions. Consequently, the specific interaction channels of relevance vary among the different experiments. Neutrino charged-current interactions can be categorized into three distinct groups based on the outcomes observed at the hadronic vertex (as depicted in Fig. 3):

- *Charged current quasi-elastic (CCQE):* At energies below $\sim$ 2 GeV, neutrino interactions involve scattering off a bound nucleon, with protons being involved in neutrino interactions and neutrons in anti-neutrino interactions. These interactions play a dominant role in the sub-GeV sample for SuperK and HyperK experiments, while also being relevant for the lowest energy bins of IceCube Upgrade and ORCA.

- *Resonance production (CC RES):* At $\sim$ 4 GeV, neutrino interactions can excite an entire nucleon, generating a baryon resonance that rapidly decays into a nucleon and one or multiple

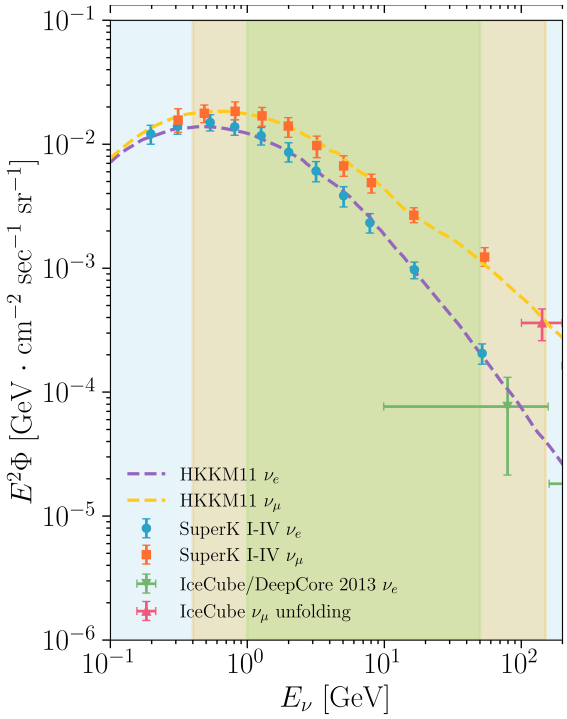

Figure 2: ***Atmospheric neutrino flux as a function of the energy.*** The total neutrino flux, measured by [10, 11], and the energy range covered by the four experiments in this analysis are depicted in the figure. Additionally, the flux prediction from the HKKM2014 model [12] is included. The top panel displays the effective volume of the three experiments as a function of neutrino energy.

mesons. These interactions are significant in all four considered experiments. Similar to CCQE, antineutrino interactions in these cases tend to produce more neutrons than protons in the final state. Additionally, the reconstruction of a Michel electron resulting from the decay of single-π^+ production aids in distinguishing between neutrinos and antineutrinos.

- *Deep inelastic scattering (CC DIS):* Above energies of $\sim$ 4 GeV, neutrinos can undergo scattering with a single quark within the nucleon, resulting in a hadronic shower in the final state. This particular channel significantly influences the neutrino interactions detected by IceCube Upgrade and ORCA.

4. Neutrino Oscillations

In the 3ν scenario, involves six parameters that describe neutrino evolution: two mass-squared differences (Δm^2_{31} and Δm^2_{21}), three mixing angles (θ_{12}, θ_{13}, and θ_{23}), and a complex phase that parameterizes the violation of the CP-symmetry in the lepton sector. Recent global analyses have determined most of these parameters at the percent level of precision [13]. However, there remain significant uncertainties for several parameters. θ_{23} can take values above and below maximal mixing within 1σ; the mass ordering shows a 2σ preference for normal ordering (NO); and δ_{CP} has a small region around $\pi/2$ excluded by T2K and SuperK at 3σ CL.

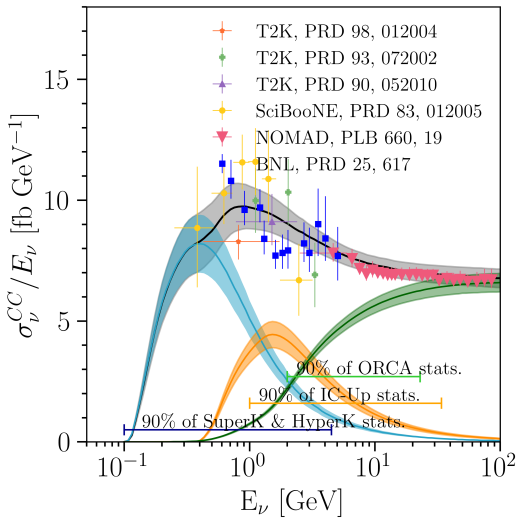

Figure 3: ***Charged-current ν_μ cross section per nucleon as a function of the neutrino energy.*** The cross section models used are from GENIE pre-computed splines, shaded regions correspond to the 1σ uncertainties considered in this work.

The large range of baselines and energies covered by atmospheric neutrinos ensures the access to a vast neutrino oscillation phenomenology. The asymmetry between neutrino and anti-neutrino oscillation is characterized by the Jarlskog invariant defined as $J = \Im[U_{\alpha i}U^*_{\alpha j}U^*_{\beta i}U_{\beta j}] = J_r \sin\delta_{CP}$. In vacuum, the CP-violation term is given by

$$P_{CP} = -8J_r \sin\delta_{CP} \sin\Delta_{21} \sin\Delta_{31} \sin\Delta_{32}, \tag{1}$$

In the sub-GeV region, the effects of δ_{CP} over neutrino evolution is enhanced due to the developement of the Δm^2_{21} term [14] and the average of Δm^2_{32} and Δm^2_{31} terms.

At the GeV scale, when neutrino trajectories pass through the Earth's mantle, there is an increase in the effective mixing angle $\tilde{\theta}_{13}$ due to the elastic interaction of the ν_e with the electrons in the Earth, the so-called MSW effect [15, 16]. For energies $\sim$ 6 GeV and densities of approximately 5g/cm^3, $\sin 2\tilde{\theta}_{13}$ reaches its maximum value, leading to a significant enhancement of flavor conversion. These resonant effects occur during neutrino (or anti-neutrino) evolution when the mass ordering is normal (or inverted).

In the multi-GeV scale, the dominant factors are Δm^2_{31} and θ_{23}. The first oscillation minimum for $P(\nu_\mu \to \nu_\mu)$ occurs at $E \sim 20$ GeV for baselines crossing the Earth. The specific energies at which this oscillation minimum happens depend on $|\Delta m^2_{31}|$, while amplitude is controlled by $\sin^2 2\theta_{23}$. The determination of the octant of θ_{23} can be achieved by measurement the electron appearance, and the matter effect in the $P(\nu_\mu \to \nu_\mu)$ which breaks the dependence on $\sin 2\theta_{23}$.

5. Experimental Analyses

To assess the sensitivity to neutrino oscillation parameters, we generate an Asimov dataset for each experiment and conduct a combined fit to the Monte Carlo simulation. This analysis involves

considering various values of the oscillation parameters, which are sampled from two separate 4-dimensional grids (Δm^2_{31}, θ_{23}, θ_{13}, and δ_{CP}). One grid corresponds to each neutrino ordering.

In our analysis, we include four experiments: SuperK [17], IceCube Upgrade [18], ORCA [19], and HyperK [20]. Within SuperK, we account for three distinct phases: SuperK without H-neutron tagging (SuperK), SuperK with H-neutron tagging (SK-Htag), and SuperK with gadolinium (SKGd). These phases are treated as independent data-taking experiments with uncorrelated detector systematics. We assume full data-taking periods from SuperK-I to SuperK-V in terms of exposure. For SKGd, we project a five-year operation with a final concentration of 0.2% gadolinium dissolved in water, starting in 2025. For the soon-to-be-deployed IceCube Upgrade and ORCA, we conservatively anticipate five and three years of operation, respectively, starting in 2025 and 2027. Regarding HyperK, we assume 2.5 years of operation beginning in mid-2027, as planned by the collaboration. As a result, our combined analysis incorporates all available atmospheric neutrino data until 2030.

6. Results

The oscillation lenght becomes comparable to the Earth size at $E_\nu \sim\sim$ 100GeV and lower. The first oscillation minimum in the muon-survival probability is located at $\sim$ 20GeV and depends on Δm^2_{31}, and the amplitude of that oscillation is controlled by $\sin^2 2\theta_{23}$. IceCube Upgrade and ORCA will provide extensive statistics for measuring the multi-GeV region of the atmospheric neutrino flux. The good angular resolution of the track sample enable a sensitivity of 0.5% for Δm^2_{31}. In the case of $\sin^2\theta_{23}$, the muon disappearance can separate between maximal mixing or not. To resolve the octant, we need to include the ν_e and ν_τ appearance, that are proporcional to $\sin^2\theta_{23}$. The better angular resolution shown by water cherenkov detectors makes ORCA able to resolve the octant. The combined analysis of all the experiments allows the exclusion of the wrong octant at more than 3σ. See Fig. 4 for a comparison between our results, the present status, and the future predictions for the next generation of neutrino experiments.

Atmospheric neutrinos shows undergo resonant flavor conversion around 6 GeV when their trajectories intersect the Earth's mantle. This resonance occurs in neutrino propagation for normal mass ordering or for anti-neutrinos with inverted ordering. In the case of IceCube Upgrade, tracks events, benefiting from improved angular resolution, exhibit a large sensitivity to this effect. For water-based experiments, the e-like and cascade samples gives the largest sensitivity to the mass ordering. By combining all the experiments, we can reach 6σ rejection of the wrong ordering for any value of $\sin^2\theta_{23}$ within the present 90% C.L. range: see Fig. 4.

The large impact that θ_{13} has at the GeV scale bring us the oportunity to measure that parameter in a complementary way to reactor experiments. Similar to the mass ordering, the largest sensitivity comes from the cascades measured in ORCA below 10 GeV, where electron neutrinos dominate. Atmospheric neutrinos provide a 20% sensitivity in determining $\sin^2\theta_{13}$ can be reached with atmospheric neutrinos: see Fig. 4. The measurement of the flavor resonant conversion will mark the first direct observation of the MSW effect occurring within the Earth.

The CP-phase remains the least constrained parameter, with nearly the entire range being allowed within a 3σ uncertainty. The large effect of δ_{CP} in the sub-GeV part of the atmospheric flux lead to SuperK and HyperK to dominate the sensitivity over this parameter rejecting part of

the parameter space at 2σ. IceCube Upgrade and ORCA, with their low-energy measurements and large statistics, can achieve a 1σ. As despicted in Fig 4, the combined analysis allow us to reach a 30% of sensitivity over δ_{CP}, and exclude regions of the parameter space to more than 3σ. The CP-phase is the parameter that benefit most of the combined analysis due to the constraints of the atmospheric flux uncertainties by IceCube Upgrade and ORCA.

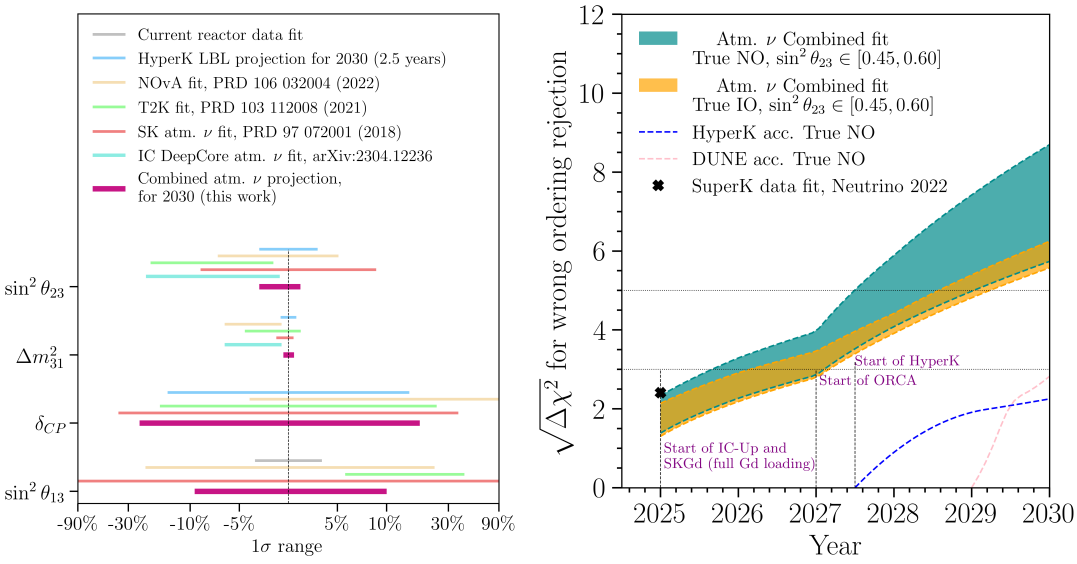

Figure 4: ***Present and future sensitivities for the neutrino oscillation parameters.*** In the left plot, we compare the 1σ regions of present experiments (T2K [21], NOvA [22], SuperK [23] atmospheric neutrinos, DeepCore [24] atmospheric neutrinos, and reactor experiments) with the projected sensitivity of Hyper-Kamiokande's accelerator program for 2030 and the combined analysis of atmospheric neutrinos in this work. The right plot shows the sensitivity in rejecting the wrong ordering, considering normal or inverted as the true scenario. The width of the bands represents the currently allowed values for $\sin^2\theta_{23}$. HyperK and DUNE [25] predictions are also included for comparison.

7. Conclusion

In this article, we examined the sensitivity of current and upcoming water(ice)-Cherenkov atmospheric neutrino detectors, specifically IceCube Upgrade, ORCA, and SuperK. Through a comprehensive study, we demonstrated the potential of a combined data-fit from these experiments, highlighting the ability to achieve precision at the few-percent level for measuring remaining oscillation parameters, including θ_{23} and Δm^2_{31}, as well as determining the neutrino mass ordering. Additionally, we emphasize that this combined analysis provides an independent constraint on the CP-phase, separate from long-baseline neutrino experiments. The results obtained from a combined fit of atmospheric neutrinos would offer valuable insights for the next-generation neutrino physics program.

References

[1] C. A. Argüelles, P. Fernández, I. Martínez-Soler, and M. Jin.

[2] G. Altarelli and F. Feruglio *Rev. Mod. Phys.* **82** (2010) 2701–2729.

[3] M. Fukugita and T. Yanagida *Phys. Lett. B* **174** (1986) 45–47.

[4] **KATRIN** Collaboration, M. Aker *et al. Nature Phys.* **18** no. 2, (2022) 160–166.

[5] **GERDA** Collaboration, M. Agostini *et al. Phys. Rev. Lett.* **120** no. 13, (2018) 132503.

[6] E. Di Valentino, S. Gariazzo, and O. Mena *Phys. Rev. D* **104** no. 8, (2021) 083504.

[7] T. K. Gaisser and M. Honda *Ann. Rev. Nucl. Part. Sci.* **52** (2002) 153–199.

[8] **Super-Kamiokande** Collaboration, T. Futagami *et al. Phys. Rev. Lett.* **82** (1999) 5194–5197.

[9] K. J. Kelly, P. A. N. Machado, I. Martinez-Soler, and Y. F. Perez-Gonzalez *JHEP* **05** (2022) 187.

[10] **IceCube** Collaboration, M. G. Aartsen *et al. Phys. Rev. Lett.* **110** no. 15, (2013) 151105.

[11] **Super-Kamiokande** Collaboration, E. Richard *et al. Phys. Rev. D* **94** no. 5, (2016) 052001.

[12] M. Honda, M. Sajjad Athar, T. Kajita, K. Kasahara, and S. Midorikawa *Phys. Rev. D* **92** no. 2, (2015) 023004.

[13] I. Esteban, M. C. Gonzalez-Garcia, M. Maltoni, T. Schwetz, and A. Zhou *JHEP* **09** (2020) 178.

[14] K. J. Kelly, P. A. Machado, I. Martinez Soler, S. J. Parke, and Y. F. Perez Gonzalez *Phys. Rev. Lett.* **123** no. 8, (2019) 081801.

[15] L. Wolfenstein *Phys. Rev. D* **17** (1978) 2369–2374.

[16] S. P. Mikheyev and A. Y. Smirnov *Sov. J. Nucl. Phys.* **42** (1985) 913–917.

[17] **Super-Kamiokande** Collaboration, Y. Fukuda *et al. Phys. Rev. Lett.* **81** (1998) 1562–1567.

[18] **IceCube** Collaboration, A. Ishihara *PoS* **ICRC2019** (2021) 1031.

[19] **KM3Net** Collaboration, S. Adrian-Martinez *et al. J. Phys. G* **43** no. 8, (2016) 084001.

[20] **Hyper-Kamiokande** Collaboration, K. Abe *et al.*

[21] **T2K** Collaboration, K. Abe *et al. Phys. Rev. D* **103** no. 11, (2021) 112008.

[22] **NOvA** Collaboration, M. A. Acero *et al. Phys. Rev. D* **106** no. 3, (2022) 032004.

[23] **Super-Kamiokande** Collaboration, K. Abe *et al. Phys. Rev. D* **97** no. 7, (2018) 072001.

[24] **IceCube** Collaboration, R. Abbasi *et al.*

[25] **DUNE** Collaboration, B. Abi *et al.*